Gibbs Energy Approach for Aqueous Processes with HF, HNO$_3$, and CO$_2$–CaCO$_3$

Justin Salminen, Petri Kobylin, and Simo Liukkonen
Helsinki University of Technology, Laboratory of Physical Chemistry and Electrochemistry, P.O. Box 6100,
FIN-02015 HUT, Finland

Osvaldo Chiavone-Filho
Universidade Federal do Rio Grande do Norte (UFRN), Departamento de Engenharia Química NT/Campus Universitário,
Natal, 59072-970, RN, Brazil

Chemical thermodynamic calculations were used to represent vapor–liquid equilibria and chemical equilibria for aqueous systems with HF, HNO$_3$, and CO$_2$–H$_2$O–CaCO$_3$ solutions. The entropy production related to the dissolution reaction of calcite was calculated using multiphase thermodynamics and experiments carried out in this work. Modern simulation methods combined with experiments provide a useful tool for the research and design of new processes as well as evaluating changes in the operational conditions of chemical processes. These methods are used to study metallurgical, pulp, and paper industrial processes that involve the presented aqueous solutions. © 2004 American Institute of Chemical Engineers AIChE J, 50: 1942–1947, 2004
Keywords: Gibbs energy, reaction, aqueous, multiphase, entropy

Introduction

Chemical thermodynamics provides a fundamental and widely applicable tool for process calculations. It has been proven able to successfully treat multiphase, multicomponent solutions, including chemical reactions. Modern computer-aided calculation methods provide useful and practical solutions for industrial and environmental processes. Today processes have grown into highly technically integrated systems where best available techniques have to be adopted to produce an environmentally acceptable, energy-efficient process. The Gibbs energy approach shows the natural boundaries of the physical and chemical interactions as contributors in different chemical environments. Simulation methods together with laboratory experiments, pilot- and mill-scale experience form an essential part in the research and design of new processes or changes in process chemistry. In this work, calculation exam-

ples are presented for industrially interesting aqueous HF, HNO$_3$, and CO$_2$–CaCO$_3$ solutions. In these systems, the knowledge of both vapor–liquid equilibrium (VLE) and chemical reactions are needed. The Gibbs energy calculation methods presented in this work can be used in some cases for the evaluation of dynamic chemical systems and systems that are kinetically constrained.

Gibbs energy approach for the calculation

Chemical and energy changes in macroscopic systems can be calculated simultaneously using multicomponent equilibrium routines including minimization of the Gibbs energy. Both the sound standard-state data and activity coefficient model, dependent on temperature, pressure, and composition, are required. The chemical potentials of pure species are derived through the tabulated values of the enthalpy of formation, heat capacity, and the entropy of formation. The total Gibbs energy of a system is constructed by summing the chemical potential μ_i for each species i. The total Gibbs energy of the multiphase system is a sum over all the stable phases that exist in the system, as follows

Correspondence concerning this article should be addressed to J. Salminen at justin.salminen@hut.fi.
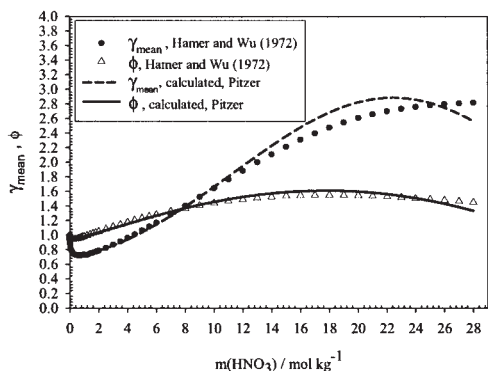
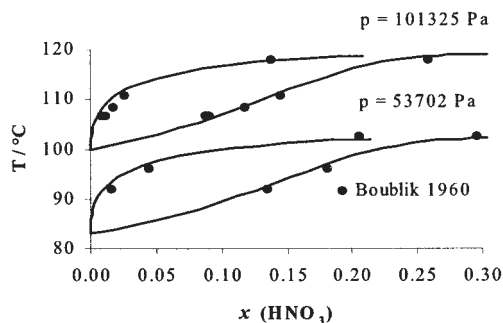**Figure 1. Calculated and measured osmotic and activity coefficient data for HNO_3 at 25°C.**

Figure 2. Vapor–liquid equilibrium diagram for HNO_3–H_2O system showing the azeotropic point. (●) Boublik and Kuchynka (1960); (—) Pitzer model.

$$G = \sum_{\alpha} \sum_{i} n_i^{\alpha} \mu_i^{\alpha} \qquad (1)$$

The Gibbs energy G of a mixture in different phases is made up of contributions of the pure components and the mixing effects, including activity terms. The chemical equilibrium in a closed system, at constant temperature and pressure, is achieved at the minimum of the total Gibbs energy, $\min(G)$, satisfying the material balance conditions. Both accurate temperature-dependent standard-state data and an appropriate activity coefficient model are required. In addition, a computer-aided calculation method is needed for evaluation of the individual compositions in the specified multiphase solution. The solution matrix of the $\min(G)$ yields the intensive properties such as concentrations and extensive state properties. The quantitative modeling of the phase and chemical equilibrium in multiphase systems constitute a key step toward the understanding and optimization of conditions used for industrially significant chemical processes.

Modeling acid solutions relevant to pickling of stainless steel

Gibbs energy minimization methods have traditionally been used for quantitative estimation of metal and mineral processing systems (Eriksson and Hack, 1990; Hack, 1996; Kobylin, 2002; Köningsberger and Eriksson, 1999; Koukkari and Liukkonen, 2002; Roine, 1999). In natural systems the acid concentrations are typically in the dilute region and the process solution can be concentrated. Mixed acid is used, for example, in the pickling process to improve the quality of steel products. Pickling is needed to remove the metal oxides formed in the surface of the steel in high-temperature annealing. The main acids in the mixed acid solution are HF and HNO_3. Knowledge of these acids in the pickling solution is essential for the process development. The mean activity coefficient and the osmotic coefficient of aqueous HNO_3 solution are shown in Figure 1, together with reference data (Hamer and Wu, 1972). The Pitzer parameters $\beta^{(0)} = 0.0979$, $\beta^{(1)} = 0.4883$, and $C^{\phi} = -0.0027$ for HNO_3 were obtained by optimization at 25°C and used in the Gibbs energy minimization calculations.

The Pitzer equation gives good results up to $x(HNO_3) = 0.2$ [14 mol/kg(H_2O)] for the HNO_3 system. For aqueous HNO_3 the vapor–liquid data are presented in Figure 2. Two parameter temperature-dependent functions for Pitzer parameters were fitted against azeotropic data (Boublik and Kuchynka, 1960). The obtained parameters, where T is in Kelvin, are: $\beta^{(0)} = -0.0004 + 29.2939$ (K/T), $\beta^{(1)} = 0.4115 + 22.9161$ (K/T), and $C^{\phi} = -0.0014 - 0.3962$ (K/T). The results are shown in Figure 2. The Pitzer activity coefficient model fails beyond the azeotropic point at $x = 0.3$.

Other models, such as Extended UNIQUAC, have also been used for the nitric acid system. The advance of this model is that, in principle, it can be applied over the full mole fraction range (Sander et al., 1986) and in some systems it can be used in aqueous mixed-solvent solutions (Chiavone-Filho and Rasmussen, 2000). The general difficulty is to relate the measured VLE properties and true chemical speciation in the liquid and gas phases. A calculation example using the minimization of Gibbs free energy for aqueous hydrogen fluoride system is shown. The reaction equations for the HF–H_2O solution is expressed as follows

$$HF(g) \Leftrightarrow HF(aq) \qquad (2)$$

$$HF(aq) \Leftrightarrow H^+ + F^- \qquad (3)$$

$$HF(aq) + F^- \Leftrightarrow HF_2^- \qquad (4)$$
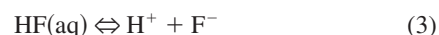
In the calculation for the aqueous HF solutions, the concept of system components is applied, as described for the system F^-–HF_2^-–H^+–OH^-–HF. In this case the formation of complex HF_2^- is taken into account in the model. In this low-pressure example the association of HF molecules in the gas phase was not taken into account. The thermodynamic data used in the model for the HF–H_2O system are shown in Table 1, including

Table 1. Thermodynamic Values for HF–H_2O System

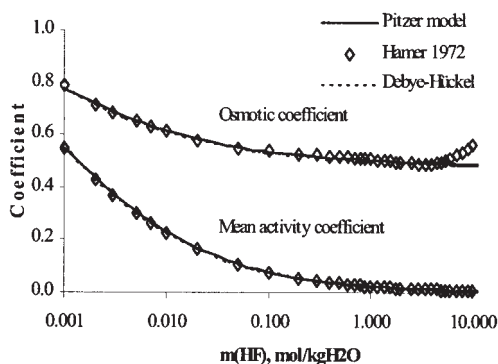|	Barner HF(aq)	Wagman HF_2^-	Wagman F^-
$\Delta_f H°$, J mol^{-1}	−320,076.0	−649,940.0	−332,630.0
$S°$, J mol^{-1} K^{-1}	88.70	92.50	−13.180
Reference	This work	Haung	Hefter/Cherif*
K_3	0.0007005	0.000612	0.000661
K_4	2.7210264	3.8601267	0.002141*

Figure 3. Calculated and measured osmotic and activity coefficient data for HF at 25°C.

reference data for the equilibrium constants K_3 and K_4 provided by Haung (1989), Hefter (1984), and Cherif et al. (2002).

The definitions for the equilibrium constants K_3 and K_4, which represent reactions 3 and 4, are given as follows

$$K_3 = \frac{a_{H^+}a_{F^-}}{a_{HF(aq)}} = \frac{m_{H^+}\gamma_{H^+}m_{F^-}\gamma_{F^-}}{m_{HF(aq)}\gamma_{HF(aq)}} \quad (5)$$

$$K_4 = \frac{a_{HF_2^-}}{a_{HF(aq)}a_{F^-}} = \frac{m_{HF_2^-}\gamma_{HF_2^-}}{m_{HF(a)}\gamma_{HF(a)}m_{F^-}\gamma_{F^-}} \quad (6)$$

where m is molality, a is activity, and γ is the activity coefficient.

The multiphase model calculates the individual activities of the aqueous species and the values for the appropriate equilibrium constants can be formed from these data. The calculations give good results up to about 10 mol/kg(H$_2$O) for the HF system. HF is a weak acid and thus the contribution of the extended Debye–Hückel model is sufficient to produce the curves presented in the Figures 3 and 4. The osmotic coefficient, mean activity coefficient, and the complex distribution of HF in aqueous solution are obtained as a result of the model calculations. Both ChemSage and ChemSheet were used to carry out the calculations and Figures 3 and 4 were produced using ChemSheet Excel spreadsheet features.
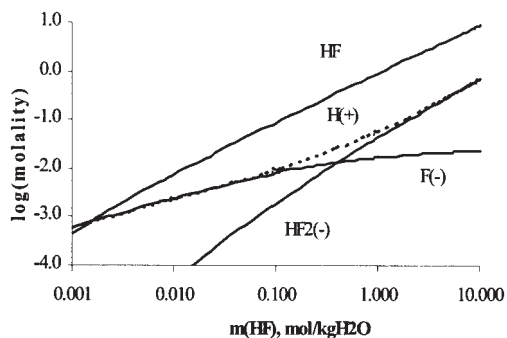

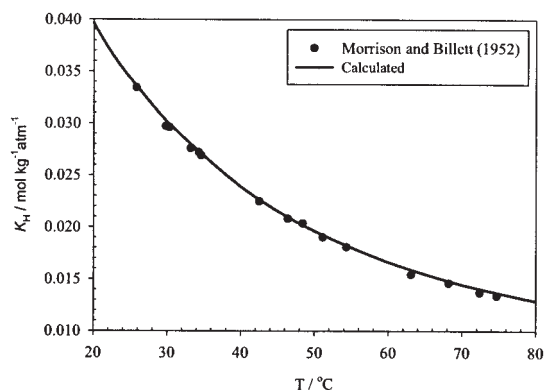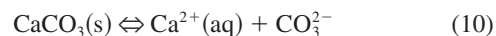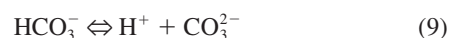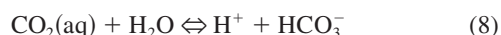**Figure 4. Calculated complex distribution for aqueous HF solution at 25°C.**

Figure 5. Equilibrium constant $K_H = a(CO_2,aq)/p(CO_2)$ for the reaction $CO_2(g) \Leftrightarrow CO_2(a)$ within 20–80°C.

The model values are compared with the solubility data of Morrison and Billett (1952).

Multiphase thermodynamics for aqueous CaCO$_3$–CO$_2$ system

The multiphase thermodynamics provide a valuable method for the estimation of the chemical states that are involved in modern pulp and paper processes. These processes are developed in the way that require an ever-smaller input of added chemicals, fresh water and simultaneously increased amount of recirculated water, wood fibers, and chemicals. Calcium carbonate is used as a filler in making fine paper grades. Recycling of calcium-containing paper influences the acid–base chemistry of the papermaking process (Koukkari et al., 2001). Carbon dioxide (CO$_2$) gas can be used as an alternative reactive acidifying chemical instead of sulfuric acid at the wet end of a paper machine in calcite-buffered solutions typically including 1–2 wt % of fibers (Pakarinen and Leino, 2000). The knowledge of the relations of pH, chemical composition, partial pressure of CO$_2$, and precipitation and dissolution of solids is mandatory. This is a reactive multiphase system that can be quantitatively treated by chemical thermodynamics. The reaction equations for aqueous CO$_2$–CaCO$_3$ system are expressed as follows

$$CO_2(g) \Leftrightarrow CO_2(aq) \quad (7)$$

$$CO_2(aq) + H_2O \Leftrightarrow H^+ + HCO_3^- \quad (8)$$

$$HCO_3^- \Leftrightarrow H^+ + CO_3^{2-} \quad (9)$$

$$CaCO_3(s) \Leftrightarrow Ca^{2+}(aq) + CO_3^{2-} \quad (10)$$
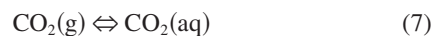
In this gas–liquid–solid system, all the phases are involved in the chemical reaction and chemical equilibrium. The numerical values of the equilibrium compositions of the chemical reactions and also pH $= -\log(a_H^+)$ values are determined through the multiphase thermodynamic model at the minimum of the Gibbs free energy. The temperature-dependent equilibrium constants for the reaction equations above are presented in Figures 5–8. The calculated equilibrium constants are obtained from composition data at the minimum of the Gibbs energy,
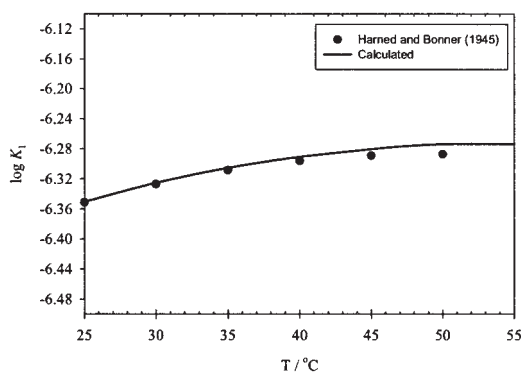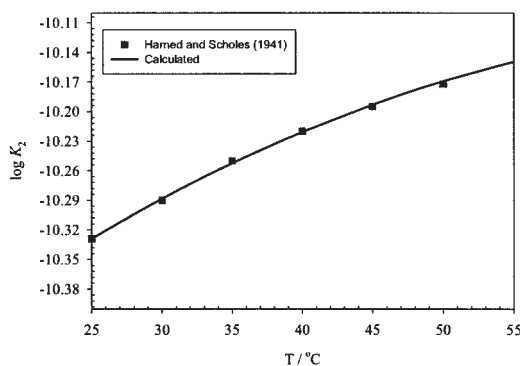
Figure 6. Equilibrium constant log K_1 for the reaction $CO_2(aq) + H_2O \Leftrightarrow H^+ + HCO_3^-$ within 25–55°C.

The calculated results are shown with reference data of Harned and Bonner (1945).

thus justifying the validity of the input data of the model. The NBS thermochemical data of Wagman (1982) were used as input data in the Gibbs energy minimization routine in the calculations, to produce the curves in Figures 5–7.

Systems that are strictly nonequilibrium processes can additionally be evaluated by the Gibbs energy approach on a point-by-point basis (Sandler, 1999). The physical and chemical changes of the fluid properties should be measurable at each time point. In the model calculations all the system state properties are defined in this dynamic chemical state that represents local equilibrium of the reactive solution. The question of how fast the reaction is cannot be answered by means of thermodynamics, and is a matter of chemical kinetics. Within the framework of the applicability of the thermodynamics, one can relate the time-dependent changes to measurable quantities (Kondepudi and Prigogine, 1998). The necessary, but not sufficient, requirement is that the standard state data and the activity coefficient model are valid within the temperature, pressure, and composition range in equilibrium. Traditionally, the Gibbs energy change $\Delta_r G$ in chemical reaction is related to the extent of reaction ξ (that is, related to the sum of chemical potentials of the reactants and products multiplied by the stoichiometric number). At equilibrium, the Gibbs energy is at the minimum, which corresponds to a zero slope in the

Figure 7. Equilibrium constant log K_2 for the reaction $HCO_3^- \Leftrightarrow H^+ + CO_3^{2-}$ within 25–55°C.

The model values are compared with the solubility data of Harned and Scholes (1941).
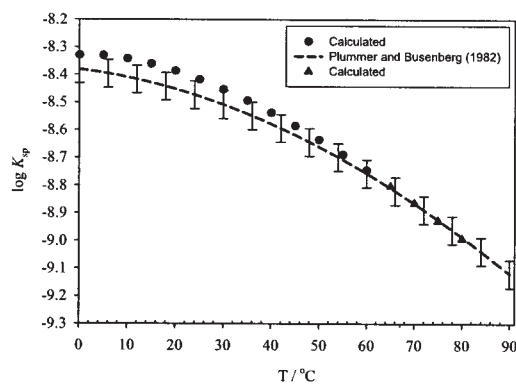
Figure 8. Solubility product of calcite $K_{sp} = a_{Ca^{2+}} a_{CO_3^{2-}}$ calculated using thermodynamic data by: ▲, Wagman (1982) NBS data; ●, heat capacity data by Shock (1988).

The experimental function, including error bars by Plummer and Busenberg (1982), is shown in the figure as a dashed line.

two-dimensional phase space, and the right-hand side of Eq. 11 is then zero

$$\left(\frac{\partial G}{\partial \xi}\right)_{T,P} = \Delta_r G = \sum_i \nu_i \mu_i \qquad (11)$$

The values of the stoichiometric coefficients are, conventionally, set positive ($\nu_i > 0$) for products and negative ($\nu_i < 0$) for reactants.

During the chemical reaction the mole amounts of chemical constituents that are involved in the reaction are changed until equilibrium is reached. The time variable enters into the thermodynamic calculation by using mass balance constraints in the model. The input mole amounts in these constraint equilibrium points are obtained using separately measured time-dependent composition of one or several components of the reactive solution (Salminen and Antson, 2002). The thermodynamic multiphase model is then applied for calculation of the rest of the intensive properties, such as compositions including pH and extensive state properties. The knowledge of some system properties can be used for evaluating other properties in the studied system. In the following experiment the dissolution reaction of $CaCO_3$ in CO_2-acidified water was studied by means of multiphase Gibbs energy model. The extended Debye–Hückel activity coefficient term, from the model proposed by Pitzer (1973), was used to describe the nonideality of the ionic species. The calculations and experiments are shown in Figures 9 and 10. The pH curves are presented for the reactive system as well as in equilibrium as a function of dissolved calcium carbonate at 25 and 50°C at total pressure 101.3 kPa. The partial pressures of CO_2 were calculated by reducing water vapor pressure from the total pressure, assuming Dalton's law to be valid. The experimental setup is as follows: 150.0 g of distilled water was charged to a glass vessel, covered, and placed in a heat bath with constant mixing, using a magnetic stirrer. The temperature of the heat bath was set within 0.1°C accuracy. The distilled water was then acidified by carbon dioxide under constant gas flow. After reaching solubility equilibrium of carbon dioxide, 100 mg of solid $CaCO_3$ (Baker,
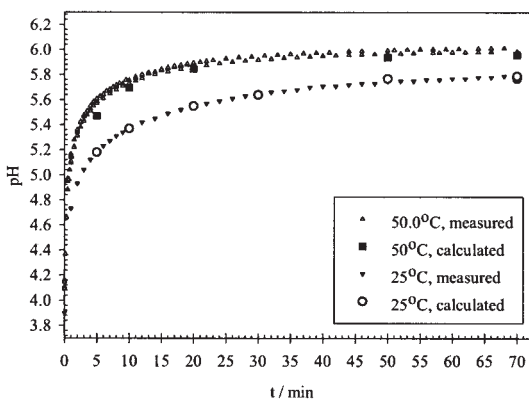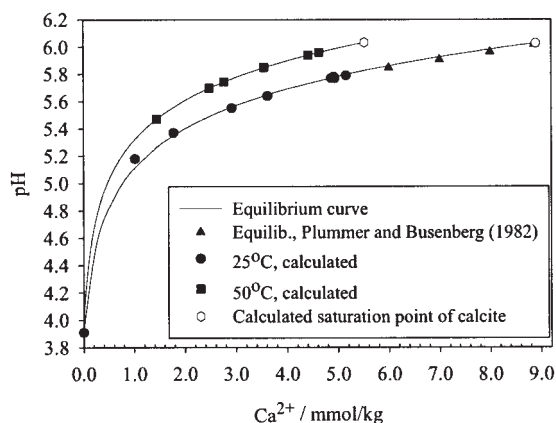
Figure 9. Calculated and measured pH values as a function of time at 25 and 50°C in 101.3 kPa total pressure.

Independent AAS analyzed Ca^{2+} data were used in the model for pH calculations.

Figure 11. Decrease of the Gibbs energy of the system in the calcite dissolution process at 25 and 50°C.

The points represent the kinetically constrained Ca^{2+} chemical amount that is allowed to react. The G is a contribution of all species over all phases and is proportional to the volume of the system. As the dissolution process of $CaCO_3$ proceeds, the G is shown to decrease toward the global minimum of the reactive system.
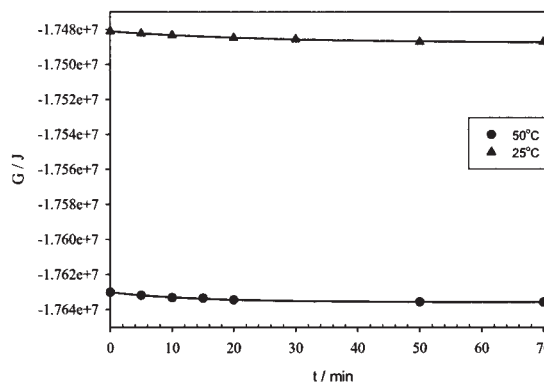
purity > 99.0%) was weighed and added to the water solution. The pH was measured online by a Metrohm 713 pH meter using combined pH glass electrode (model 6.0238.00). The electrodes were calibrated with standard buffer solutions before each experiment at the temperature of the experiment. The Ca^{2+} content was analyzed from samples taken in different time points by atomic adsorption spectrometry (AAS). These analyzed chemical amounts of Ca^{2+} were used in the Gibbs energy minimization routine as feed amounts of dissolved calcium carbonate. The calculation yields the corresponding homogeneous equilibrium in the aqueous phase with the given mass-balance constrains of Ca^{2+}, thus satisfying the electroneutrality condition at given $p(CO_2)$ and T. The calculated pH values were then compared with online pH measurements at the same time point as the dissociation reaction of calcium carbonate advances toward saturated solution.

The equilibrium calculations can provide information on the system if the chemical changes are relatively slow. The time constant of the pH tip-point electrode is small compared to the

reaction rate, and the samples taken are assumed to represent the state of the system at the time point considered. The $CaCO_3$ dissolution shown in Figures 9 and 10 strictly concerns nonequilibrium processes that can be calculated by the Gibbs energy approach using material-balance restrictions for Ca^{2+} species. Each time point is related to the model calculation by the boundary conditions that are specific for the problem. At each time point, all the system state properties are defined for each step of given feed amounts. In Figures 11 and 12, the corresponding Gibbs energy change and the entropy production are shown. For a closed system at constant temperature and pressure, the entropy production is expressed as the time derivative of the Gibbs energy function. In this case, the entropy change d_iS is attributed to the chemical changes of the closed system. The Gibbs energy should be a decreasing function and the entropy production positive for natural changes. The relations for entropy production, in a system without heat and mass exchange with the system and the surroundings, are shown in Eqs. 11 and 12 (Kondepudi and Prigogine, 1998). The entropy

Figure 10. Calculated and measured pH values as a function of Ca^{2+} amount at 25 and 50°C in 101.3 kPa total pressure.

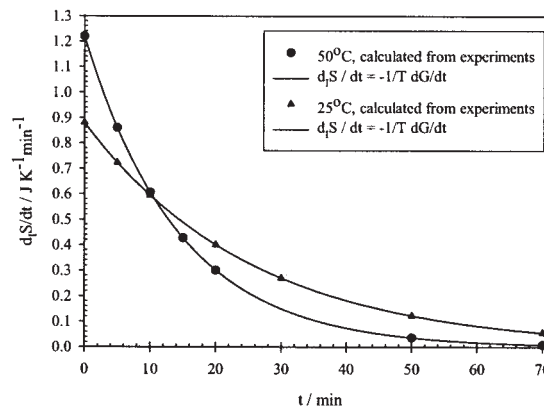The results of the dynamic measurements and equilibrium values by Plummer and Busenberg (1982) are also shown.

Figure 12. Entropy production during the dissolution process at 25 and 50°C.

production in this system is assumed to result from the chemical reaction that can be expressed through chemical potentials

$$d_I S = -\frac{1}{T}\sum_i \mu_i d_i n_i \qquad (12)$$

$$\frac{d_I S}{dt} = -\frac{1}{T}\frac{dG}{dt} \qquad (13)$$

The calculations are thermodynamically consistent, given that the G value decreases during the dissolution reaction and the entropy production at constant temperature remains positive and approaches zero as the reaction proceeds toward equilibrium. The curves in Figure 12 show that at 50°C the dissolution process is faster than that at 25°C, which is in accordance with the fact that the solubility of $CaCO_3$ is lower at 50°C than at 25°C, and at 70 min the equilibrium is closer for the reaction that occurs at 50°C.

Discussion and Conclusions

The advantages of using the Gibbs energy approach are that the extensive state properties are well defined and tested and have firm scientific basis. Furthermore, it allows simultaneous evaluation of the multicomponent, multiphase solution including chemical reaction. Knowledge of both the equilibrium and the nonequilibrium chemistry of aqueous CO_2–$CaCO_3$ systems is important because these appear both in environmental systems and in industrial processes. The general Gibbs energy method can be further extended for specific dynamic processes that are usually treated by means of chemical kinetics. Dynamic constraints, such as material restrictions, can be included in the model for specific systems, giving additional value for the calculations based on the state functions and classical thermodynamics. The modern computer-aided multicomponent and multiphase calculation methods are rigorous methods for studying industrial processes that concern aqueous solutions. The pulp, paper, and metallurgical industries are fine examples of the successful integration of new methods into practice.

Literature Cited

Barner, H. E., and R. V. Scheuerman, *Handbook of Thermochemical Data for Compounds and Aqueous Species*, Wiley, New York, 156s (1978).

Boublik, T., and K. Kuchynka, "Gleichgewicht Flüssigkeit-dampf XXII. Abhängigkeit der Zusammensetzung des Azeotropischen Gemisches des Systems Salpetersäure–Wasser vom Druck," *Collect. Czech. Chem. Commun.*, **25**, 579 (1960).

Cherif, M., A. Mgaidi, M. N. Ammar, M. Abderrabba, and W. Fürst, "Representation of VLE and Liquid Phase Composition with an Electrolyte Model: Application to H_3PO_4–H_2O and H_2SO_4–H_2O," *Fluid Phase Equilibria*, **194–197**, 729 (2002).

Chiavone-Filho, O., and P. Rasmussen, "Modelling Salt Solubilities in Mixed Solvents," *Brasilian J. Chem. Eng.*, **7**(2), 117 (2000).

Erikson, G., and K. Hack, "Chemsage—A Computer Program for the Calculation of Complex Chemical Equilibria," *Met. Trans. B*, **21B**, 1013 (1990).

Hack, K., *The SGTE Casebook, Thermodynamics at Work*, Materials Modelling Series, The Institute of Materials, Borne Press, Bournemouth, UK (1996).

Hamer, W. J., and Y. C. Wu, "Osmotic Coefficients and Mean Activity Coefficients of Univalent Electrolytes in Water at 25°C," *J. Phys. Chem. Ref. Data*, **1**, 1047 (1972).

Harned, H., and F. Bonner, "The First Ionization of Carbonic Acid in Aqueous Solutions of Sodium Chloride," *J. Am. Chem. Soc.*, **67**, 1026 (1945).

Harned, H., and S. Scholes, "The ionization constant of HCO_3^- from 0 to 50°C," *J. Am. Chem. Soc.*, **63**, 1706 (1941).

Haung, H. H., "Estimation of Pitzer's Ion Interaction Parameters For Electrolytes Involved in Complex Formation Using a Chemical Equilibrium Model," *J. Solution Chem.*, **18**, 1069 (1989).

Hefter, G. T., "Acidity Constant of Hydrofluoric Acid," *J. Solution Chem.*, **13**, 457 (1984).

Kim, H. T., and W. J. Frederick, Jr., "Evaluation of Pitzer Ion Interaction Parameters of Aqueous Electrolytes at 25°C. 1. Single Salt Parameters," *J. Chem. Eng. Data*, **33**, 177 (1988).

Kobylin, P., "Thermodynamic Modelling of Aqueous Solutions for Stainless Steel Pickling Processes," Licentiate's Thesis, Helsinki University of Technology, Finland, (2002).

Kondepudi, D., and I. Prigogine, *Modern Thermodynamics: From Heat Engines to Dissipative Structures*, Wiley, New York (1998).

Königsberger, E., and G. Eriksson, "Simulation of Industrial Processes Involving Concentrated Aqueous Solutions," *J. Solution Chem.*, **28**, 721 (1999).

Koukkari, P., and S. Liukkonen, "Calculation of Entropy Production in Process Models," *Ind. Eng. Chem. Res.*, **41**, 2931 (2002).

Koukkari, P., R. Pajarre, H. Pakarinen, and J. Salminen, "Practical Multiphase Models for Aqueous Process Solutions," *Ind. Eng. Chem. Res.*, **40**, 5014 (2001).

Koukkari, P., K. Penttilä, K. Hack, and S. Petersen, "ChemSheet—An Efficient Worksheet Tool for Thermodynamic Process Simulation," *Microstructures, Mechanical Properties and Process-Computer Simulation and Modelling*, Y. Brechet, ed., Euromat99 Vol. 3, Wiley–VCH, New York (2000).

Morrison, T., and F. Billett, "The Salting Out of Non-Electrolytes. Part II. The Effect of Variation in Non-Electrolyte," *J. Chem. Soc.*, 3819 (1952).

Pakarinen, H., and H. Leino, "Benefits of Using Carbon Dioxide in the Production of DIP Containing Newsprint," *Proc. 9th PTS-CTP Deinking Symposium*, Munich, Germany, May 9–12 (2000).

Pitzer, K. S., "Thermodynamics of Electrolytes. 1. Theoretical Basis and General Equations," *J. Phys. Chem.*, **77**, 268 (1973).

Plummer, L., and E. Busenberg, "The Solubilities of Calcite, Argonite and Vaterite in CO_2–H_2O Solution between 0 and 90°C, and an Evaluation of the Aqueous Model for the System $CaCO_3$–CO_2–H_2O," *Geochim. Cosmochim. Acta*, **46**, 1011 (1982).

Roine, A., HSC-Software v. 4.1, 88025-ORC-T, Outokumpu Research Centre, Pori, Finland (1999).

Salminen, J., and O. Antson, "Physico-Chemical Modelling of Bleaching Solution and Reaction," *Ind. Eng. Chem. Res.*, **41**, 3312 (2002).

Sander, B., A. Fredeslund, and P. Rasmussen, "Calculation of Vapour Liquid Equilibria in Nitric Acid–Water–Nitrate Salts Systems Using an Extended UNIQUAC Equation," *Chem. Eng. Sci.*, **41**, 1185 (1986).

Sandler, S., *Chemical and Engineering Thermodynamics*, 3rd Edition, Wiley, New York (1999).

Shock, E. L., and H. C. Helgeson, "Calculation of the Thermodynamic and Transport Properties of Aqueous Species at High Pressures and Temperatures: Correlation Algorithms for Ionic Species and Equation of State Predictions to 5 kbar and 1000°C," *Geochim. Cosmochim. Acta*, **52**, 2009 (1988).

Wagman, D. D., et al., "The NBS Tables of Chemical Thermodynamic Properties. Selected Values for Inorganic and C_1 and C_2 Organic Substances in SI Units," *J. Phys. Chem. Ref. Data*, **11**, 1 (1982).